

Antiviral and antioxidant activity, green synthesis, and optimization of silver nanoparticles derived from *Ulva lactuca*

**Mofida E. M. Makhlof¹, Heba A. Diab¹, Mona E. Mabrouk¹,
Mohamed S. Abd El Kareem^{2*}**

*1- Botany and Microbiology Department, Faculty of Science, Damanhour
University*

*2- Botany and Microbiology Department, Faculty of Science, Alexandria
University*

Abstract:

This article investigated the synthesis of silver nanoparticles from *Ulva lactuca* with their antiviral and antioxidant activity. The optimization of nanoparticle synthesis was also regulated. *Ulva lactuca* was collected in June 2020, prepared, and optimized for silver nanoparticle synthesis. Confirmation of the formation of the silver nanoparticles by *Ulva lactuca* aqueous extract was determined by UV–VIS spectrophotometer. The nanoparticles were found to be distinct, regular, and primarily spherical, with sizes ranging from 4.08 - 27.57nm, and the average size of particles was found to be 10.29 nm. Silver nanoparticles synthesized from *Ulva lactuca* showed significant antioxidant activity but less than conventional ascorbic acid. It also showed important cytotoxic activity against the VERO cell line but weak antiviral activity against Adenovirus. The effect of reaction time, AgNO₃ Solution to algal extract, precursor concentration, temperature, time, and pH on silver nanoparticle synthesis was evaluated. Characterization of the produced nanoparticles was also performed.

Keywords: Biological activity, green algae, nanotechnology, *Ulva lactuca*, antiviral, anticancer, optimization, silver nanoparticles.

Introduction

Nanotechnology is a unique, rapidly growing, dynamic, multidisciplinary, and innovative field of science that attracts researchers and scientists from various fields, including physicists, chemists, engineers, and biologists across the globe with potential health, environmental, and socioeconomic applications (**Mena, 2011 and 2013; Sharma et al., 2016; Batool et al., 2019; Mohanta et al., 2022**). Nanotechnology involves the synthesis, characterization, and applicability of particles with a size variation from 1–100 nm, called nanoparticles (NPs). These

*Corresponding author: email: msabdelkareem@gmail.com

NPs exhibit various new properties owing to their small size, large surface-to-volume ratio, catalytic activity, chemical stability, high conductivity, and biological properties (Nayak *et al.*, 2016; Jakinala *et al.*, 2021; Mohanta *et al.*, 2022). Due to their valuable and unique physical, chemical, and mechanical properties, NPs are widely used in a wide range of applications, including cosmetics, medications, energy, electronics, catalysis, wastewater treatment, food production, heavy metal adsorption, and agriculture (Saied *et al.*, 2021; Makhlof *et al.*, 2022).

Silver nanoparticles (AgNPs) are among the most vital and fascinating nanomaterials among several metallic nanoparticles involved in biomedical applications (Yesilot and Aydin, 2019; Karmous *et al.*, 2020). AgNPs have attracted attention due to their wide range of applications, including biosensors, drug delivery, imaging, renewable energy technologies, luminescence, optics, electronics, textiles, cosmetics, food industry, dentistry, biomedicine, and agriculture. In addition, they have been reported for antimicrobial, antioxidant, anticancer, antibacterial, and antiviral properties (Rudrappa *et al.*, 2023). Metal nanoparticles are generally synthesized using traditional chemical and physical methods, making them with desired properties such as oxidation, deposition precipitation, anodization, conventional heating, and hydrothermal methods (Badineni *et al.*, 2021). Moreover, these synthesis methods are labor-intensive, expensive, and hazardous to living organisms and the natural environment. To overcome these limitations associated with traditional methods, a production technique called "Green synthesis" has been developed, which differs from physical and chemical processes by being more environmentally friendly, economically viable, and instantly scalable for batch production. It also provides controlled growth, crystal growth, increased influence, increased stability, and uniform size (Valsalam *et al.*, 2019; Anand *et al.*, 2020; El-Sheekh *et al.*, 2020 & 2021; Makhlof *et al.*, 2022).

The current trend in the "green synthesis" of nanoparticles is utilizing algal species, including members of the Chlorophyceae, Phaeophyceae, Cyanophyceae, Rhodophyceae, and Diatoms. Biosynthesis of nanoparticles using algae is a rapidly growing approach as it is easy to handle and utilize algae. Algae have a strong ability to accumulate and absorb inorganic metallic ions, and the utilization of algae to synthesize nanoparticles represents a natural, ecofriendly, fast, and cost-effective method that has low toxicity (Tripath *et al.*, 2017; Mohanta *et al.*, 2022).

Ulva lactuca (UL), a green macroalgae that grows throughout the Mediterranean coast and is common in Egypt's north shore, belongs to the phylum Chlorophyta, class Ulvophyceae, and family Ulvaceae and is popularly referred to as "sea lettuce" (Postma *et al.*, 2018). UL aqueous extract is rich in bioactive molecules, including Ulvan polysaccharides, amides, pigments, proteins, amines, terpenes, phenols, and alkaloids, all of which have a significant role in the stabilization and reduction of metal (Rajesh *et al.*, 2012; Makhlof *et al.*, 2022). In the last years, there has been an increasing number of studies reporting on the application of UL in the synthesis of silver nanoparticles led by UL extract (Devi *et al.*, 2012; Kumar *et al.*, 2013; Valentin and Kumari, 2014; Murugan *et al.*, 2015; González-Ballesteros *et al.*, 2018).

Materials and Methods

Sample collection and preparations

In June 2020, samples of *Ulva lactuca* were manually gathered from the rocky shores of Abu Quir Bay in Alexandria, Egypt (latitudes 31° 03' and 31° 22' N and longitudes 30° 20' and 30° 25' E). The collected samples were identified according to Aleem (1978 and 1993), Lipkin and Silva (2002), and the AlgaeBase website (Guiry in Guiry 2020). All samples were taken directly and promptly

washed in seawater to remove any foreign particles, sands, or epiphytes. Then, it was placed in polythene bags filled with natural seawater and brought to the laboratory, where it was washed correctly with running tap water and then distilled water to remove any leftover, adhering particles, related biota, and sand. The algal samples were shade-dried in air, then dried in an oven (Mettler, Germany) at 60 °C for 3 h. The dried samples were ground to a fine powder with a mixer grinder (Brown mill) and stored in plastic bags at room temperature for further experiments.

Preparation of *Ulva lactuca* aqueous extract and synthesis of AgNPs

In a 500 ml Erlenmeyer flask, 10 grams of *U. lactuca* powder was added to 200 ml of distilled water. The mixture was boiled in a water bath for 30 min. at 100 °C with intermittent stirring for biomolecule extraction from an algal sample. The extract was obtained by filtration using Whatman No.1 filter paper and centrifugation at 6708g.

Optimization of operational physico-chemical parameters for AgNPs biosynthesis

Physiochemical parameters regulate the biosynthesis of inorganic metal nanoparticles to achieve optimum operation to obtain maximum product yield (Khan and Jameel, 2016; Gupta *et al.*, 2018) and to get uniform shape and size of nanoparticles. The one-factor-at-a-time (OFAT) method was applied to select the essential factors. This design depended on studying one factor while the other variables were constant. The factors employed for AgNPs synthesis include reaction time, illumination, volume ratio of the mixtures, the concentration of AgNO₃, the effect of temperature and pH values.

Reaction time

To study the influence of reaction time on the biosynthesis of AgNPs, 1 ml of algal extract was mixed with 9 ml 1 mM AgNO₃ (Sigma Aldrich, USA) at room temperature (30°C), under light conditions, origin pH (without changing the pH of the reaction) for 8, 10, 12, 24, 36, 48, 60, 72, 84, 96 and 120 h. After incubation, the suspension converted to a red-brown color, and aliquots of the samples were analyzed using UV–vis spectroscopy. The optimum reaction time was chosen based on the absorbance values of the AgNPs in the range of 400–500 nm.

Ratio change of AgNO₃ Solution to algal extract

The effect of the algal extract and precursor ratio on the synthesis of AgNPs was investigated. by mixing algal extract with AgNO₃ (1 mM) at different ratios of 1:9, 2:8, 3:7, 4:6, 5:5, 6:4, 7:3, 8:2 and 9:1 (V/V of algal extract to AgNO₃) at 30 °C, under light, and origin pH (without changing the pH of the reaction) for 84 h.

Precursor Concentrations

To study the influence of precursor concentrations on the biosynthesis of AgNPs, 5ml of algal biomass extract was mixed with 5 ml of (0.5, 1, 1.5, 2, 2.5, 3, 4, 5, 6, 7 and 8mM AgNO₃) at 30°C, under light, origin pH (without changing the pH of the reaction) for 84 h. After incubation, aliquots of the samples were analyzed using UV–vis spectroscopy.

Effect of temperature, light, and pH

A mixture of algal extract was mixed with an optimum concentration of AgNO₃ (4mM) at a 5:5 ratio and kept at 30, 40, 50, 60, and 90°C under constant light and pH. The effect of illumination on the biosynthesis of AgNPs was

examined by keeping the reaction mixture at light conditions (using LED fluorescent lamps) and dark conditions.

The variation in pH during the synthesis of AgNPs was studied by adding an algal extract to AgNO₃ and adjusting the reaction pH to be 4, 5, 6, 7, 8, 9, 10 and 11 using HCl or NaOH (0.1 M). All factors were tested in sequence. The absorbance values of the resulting solution was measured using UV-vis spectroscopy, where the absorbance intensity indicates the number of nanoparticles formed (**Ahmed *et al.*, 2013**).

Detection and purification of optimum phyco-synthesized ULAgnPs.

The optimum conditions for AgNPs synthesis were at 5 ml of algal extract 5 ml of AgNO₃ (4 mM) at 60°C, and light incubation at pH (8). After incubation, high speed centrifugation was used to separate the biosynthesized nanoparticles from the reaction mixture for 15 min. at 20124 g. After that, they were centrifuged once more after being washed with sterile distilled water. This procedure was repeated three times to generate pure nanoparticles to eliminate unreacted metals, remaining biological molecule contaminants, and any remaining metabolites from native nanoparticles (**Nagarajan and Kuppusamy, 2013; Al-kordy *et al.*, 2021**). After being cleaned with ethanol to remove any remaining ionic contaminants, the powder was dried overnight at 40°C in the oven before being described.

UV-Vis Spectroscopy

The maximum Absorbance of ULAgnPs was measured using a UV-Vis spectrophotometer (Thermo Scientific Evolution TM 300) in the wavelength range between 300 nm and 700 nm while using distilled water as a blank (**Shamsuzzaman *et al.*, 2013; Dhoble and Kulkarni, 2016**).

Transmission electron microscopy (TEM)

The size and morphology of the synthesized ULAgNPs were examined using TEM JEM- 1400 plus (JEOL, Corp., Tokyo, Japan) with an accelerating voltage of 50 kV. Deionized water was used to dilute the reaction mixture and was sonicated (Branson-Sonifier 250, Branson Ultrasonics Corp., Danbury, CT, USA) for 10 min (**Tahmasebi *et al.*, 2015**). The sonicated sample was then placed onto copper grids coated with carbon, which was then vacuum dried for 30 min before electron micrographs were taken of the sample (**Gupta *et al.*, 2018**).

Biological activities

Antiviral activity of ULAgNPs

Mammalian Cell Line

The American Type Culture Collection (ATCC, Manassas, VA, USA) provided the Vero cells (derived from the kidney of an African green monkey). Vero cells were grown in Dulbecco's modified Eagle's medium (DMEM), which included 10% heat-inactivated fetal bovine serum (FBS), 1% L-glutamine, HEPES buffer, and 50 µg/ml gentamycin. All cells were cultured twice a week and kept at 37 °C in a humidified atmosphere with 5% CO₂ (**Vijayan *et al.*, 2004**).

Virus Propagation and Antiviral Assay

The cytopathogenic Adenovirus strain 2 was propagated and tested in confluent Vero cells. The Regional Center for Mycology and Biotechnology conducted the antiviral screening (RCMB, Al-Azhar University, Cairo, Egypt). This assay was chosen to demonstrate specific inhibition of a biological function, precisely a cytopathic effect in susceptible mammalian cells measured using the MTT method (**Hu and Hsiung 1989; Al-Salahi *et al.*, 2015; Randazzo *et al.*, 2017**). The Spearman-Kärber method was used to count infectious viruses by determining the 50% tissue culture infectious dose (TCID₅₀) with eight wells per

dilution and 2 μ l of inoculum per well (**Pinto *et al.*, 1994**). In the cytotoxicity assay, the Vero cell lines were seeded in 96-well plates at a cell concentration of 2×10^5 cells per ml in 100 μ l of growth medium. After 24 h of seeding, a fresh medium with varying concentrations of ULAgNPs was added. A multichannel pipette was used to add serial two-fold dilutions of ULAgNPs (ranging from 2 μ g/ml to 3000 μ g/ml) to confluent cell monolayers dispensed into 96-well, flat-bottomed microtiter plates (Falcon, Jersey, NJ, USA). The microtiter plates were incubated for 48 h at 37 °C in a humidified incubator with 5% CO₂. Three wells were used for each concentration of the tested sample. Control cells were incubated with or without test samples and DMSO. The small amount of DMSO in the wells (maximum 0.1%) did not affect the experiment. Following the incubation period, the viable cell yield was determined using an MTT colorimetric method (**Mosmann, 1983**) and the following equation: $[(A - B)/(C - B)] \times 100\%$ where A, B, and C indicate the Absorbance of the ULAgNPs with virus-infected cells, the Absorbance of the virus control and the Absorbance of the cell control, respectively. The 50% cytotoxic concentration (CC₅₀), or the concentration required to cause toxic effects in 50% of intact cells, was calculated using GraphPad Prism software from graphic plots of the dose-response curve for each concentration (San Diego, CA, USA).

Data Analysis

The STATA modeling software calculated the dose that inhibited viral infection by 50% (EC₅₀) compared to the virus control. The percentages of viral inhibition concerning each tested virus represent the mean and standard error of the three experiments' mean values. The EC₅₀ values were calculated directly from the curve obtained by plotting the virus yield inhibition against the concentration of ULAgNPs. The selectivity index (SI) was calculated using the CC₅₀/EC₅₀ ratio to determine whether each compound had sufficient antiviral activity that outweighed

its toxicity (**Al Salahi et al., 2015**). This index, known as a therapeutic index, was used to determine whether a compound was necessary. Compounds with an SI value of 2 or higher were considered active (**Al-Salahi et al., 2015**).

DPPH (2, 2-Diphenyl-1-picryl hydrazyl) radical scavenging activity

A prepared (0.004% w/v) DPPH radical methanol solution was prepared and stored at ten °C in the dark. ULAGNPs methanol solution (2-1000 µg/ml) was designed. To 3ml of DPPH solution, a 4 µl aliquot of ULAGNPs methanol solution was added, and the mixture was vortexed vigorously and allowed to stand at 22 – 25 °C for 30 min in the dark. A UV-visible spectrophotometer was used to immediately measure Absorbance at 515 nm (Milton Roy, Spectronic 1201). The decrease in Absorbance was measured continuously, with data recorded every 1 min until the Absorbance stabilized (16 min). The Absorbance of the DPPH radical (control) and the reference compound ascorbic acid were also measured.

The DPPH radical's percentage inhibition (PI) was calculated using the formula:

$$\text{PI} = [(AC - AT) / AC] \times 100 \quad (1)$$

Where AC = Absorbance of the control at t = 0 min and AT = absorbance of ULAGNPs + DPPH at t = 16 min (**Yen and Duh 1994**). GraphPad Prism software estimated the 50% inhibitory concentration (IC₅₀), or the concentration required to achieve 50% DPPH radical scavenging activity (San Diego, CA. USA).

Results and Discussion

Biosynthesis of ULAGNPs

In this study, we revealed the green synthesis of silver nanoparticles by *Ulva lactuca*. The *Ulva lactuca* aqueous extract was mixed with silver nitrate solution, monitored, and observed for color changes. The formation of a brownish-red color indicates the biogenesis of AgNPs. It suggests the bio-reduction of Ag⁺ ions into Ag⁰, which resulted in colloidal nanoparticles (Solanki and Patel, 2022) confirmed the nanoparticle formation. Where there was no color change in the control AgNO₃ solution (Fig.1). Confirmation of the formation of the silver nanoparticles by *Ulva lactuca* aqueous extract was determined by UV–VIS spectrophotometer.

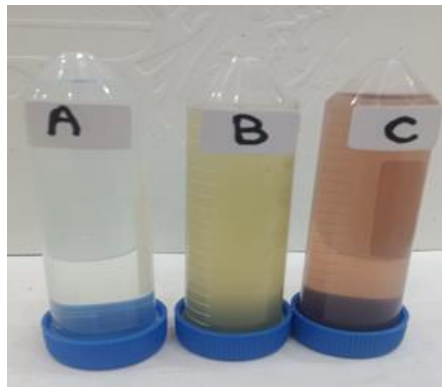


Fig. 1. Visual observations of color change before and after the conversion of Ag⁺ to Ag⁰ nanoparticles by *Ulva lactuca* aqueous extract. (A) Pure precursor salt solution (AgNO₃), (B) *Ulva lactuca* aqueous extract, (C) Brownish red color showing synthesized ULAGNPs mixing *U. lactuca* aqueous extract with AgNO₃ solution

Optimization of operational physico-chemical parameters for ULAgNPs biosynthesis

The optimization of various parameters is important in order to achieve optimum conditions where the maximum yield of nanoparticles can be obtained. UV-Vis absorption intensity was used as an indication of nanoparticles formation yield during the reaction. The absorption intensity indicates the number of nanoparticles formed (Arasu *et al.*, 2019). Several conditions, such as physical, chemical, and environmental factors, affect the biosynthesis of AgNPs with the help of algae. Some essential factors are extract or biomass concentration, pH, reaction time, illumination, precursor concentration, and temperature. These conditions must be appropriately maintained for efficient biosynthesis of silver nanoparticles as they affect the nucleation, formation of stabilized nanoparticles, the rate of production, yield, and morphologies of NPs (Shah *et al.*, 2015; Salem and Fouda, 2020).

Reaction time

Reaction time is required to reduce the metal nanoparticles (Gupta *et al.*, 2019). Reaction time is a crucial factor governing the structure and shape of AgNPs (Aldakheel *et al.*, 2023). There is an exponential increase in the Absorbance for the first 84 h (Fig. 2), in which the nucleation and the growth occurred, after that, the reduction followed a slow trend. The complete conversion of Ag^+ to Ag^0 occurred within 84h, which was evident from the gradual increase in the intensity of the brownish-red color (Fig. 3) and the absorbance values ($\text{OD } 440_{\text{nm}} \approx 1.2$) with maximum absorbance peak at 440 nm (Fig. 2). The obtained data indicate that the reaction time required for ultimate synthesis of ULAgNPs was 84h.

During the biological synthesis of NPs, three main events occur (a) the initiation of the ion reduction process, (b) the nucleation and growth of the NPs,

and (c) the complete reduction of ions. There is evidence that the initiation of the reduction process requires between 5 and 15 minutes (**Alzahrani and Welham, 2014; Rao and Tang, 2017**). Sometimes, it happens immediately after mixing the precursor salt with the biological extract (**Singh and Srivastava, 2015; Kumar *et al.*, 2016**). A complete reaction can occur between 45 and 120 minutes, depending on the reducing agent's effectiveness (**Alzahrani and Welham, 2014; Rao and Tang, 2017; Satpathy *et al.*, 2019**). However, some studies have proved that the green reactions may reach equilibrium after one week (**Dipankar and Murugan, 2012; Khalil *et al.*, 2014**). For example, **Wei *et al.* (2021)**, reported that silver NPs needed five hours to be wholly formed in a mixture of organic residues while, in *Hibiscus cannabinus* leaf extract, they became stable after five days (**Bindhu and Umadevi, 2013**). It also has been observed that **Codium capitatum** acquired around 48 hr. for the production of nanoparticles from the precursor, whereas it acquired just 30 min for synthesis by *Chaetomorpha linum* (**Kannan *et al.*, 2013; Dhavale *et al.*, 2020**).

Ratio change of AgNO₃ Solution to algal extract

The volume ratio of the algal extract and metal solution is one of the most important factors that influence the biosynthesis of AgNPs. It has been observed that the volume ratio of the algal extract and metal solution is directly related to the yield of nanoparticles. In addition, these ratios significantly influence the size and structure of nanoparticles (**Rahman *et al.*, 2020**).

In these experiments, different volume ratios of algal extract to precursor solution (AgNO₃) were optimized to increase the formation of AgNPs. The highest SPR peak (OD_{400nm} ~ 2.7) was obtained with a volume ratio of **5:5** (algal extract to AgNO₃) (**Fig. 4 and 5**).

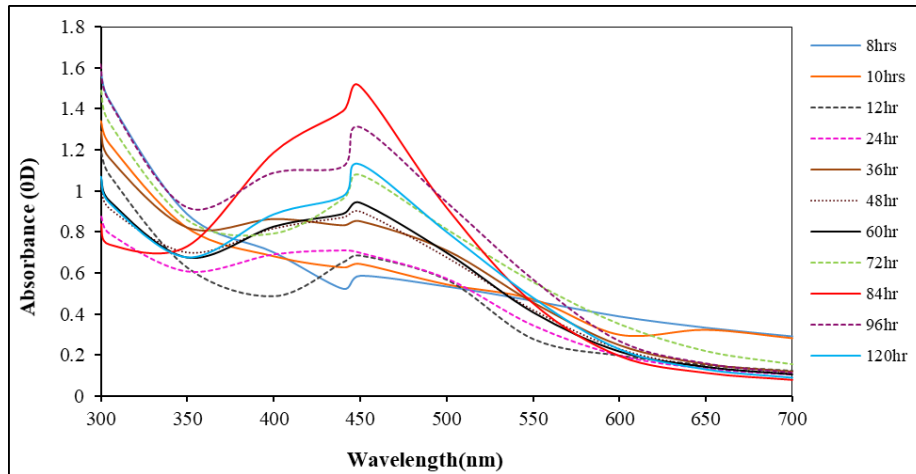


Fig. 2. UV-Vis spectra showing the effect of reaction time for efficient biosynthesis of ULAgNPs



Fig. 3. Biosynthesis of ULAgNPs kept at different incubation time intervals at static conditions at 30°C.

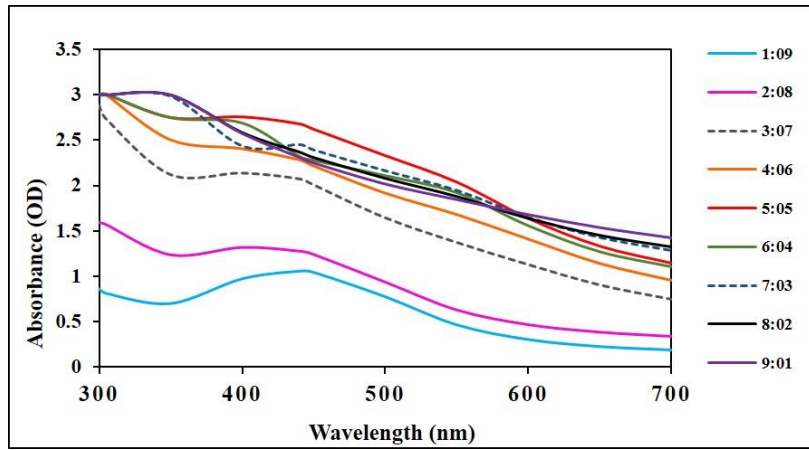


Fig. 4. UV- Vis spectra of ULAGNPs at different volume ratios of algal extract and AgNO₃

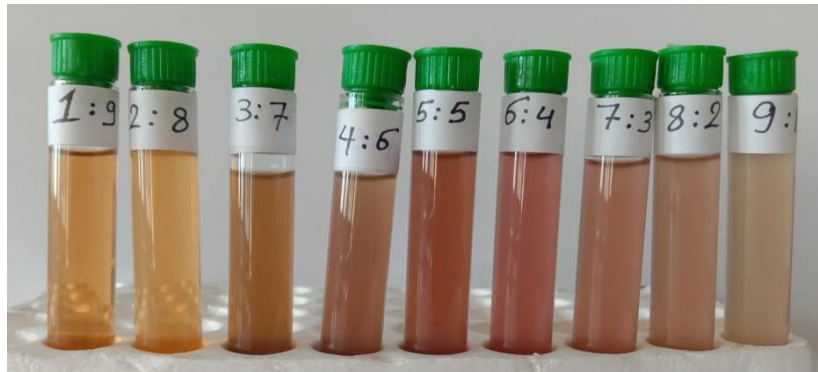


Fig. 5. Biosynthesis of ULAGNPs with different ratios of algal extract and 1mM AgNO₃ at static conditions and 30 °C for 84 h.

This could be attributed to the sufficient amount of reductants reacted with silver ions. As concentration increases, higher numbers of stable nuclei are formed due to sufficient reductants reacting with silver ions.

However, nucleation occurs faster at higher concentrations, and unstable nuclei formed react with free silver ions in the reaction mixture, resulting in large-sized silver nanoparticles reducing UV absorption capability (**Verma et al., 2016**).

This result is in good agreement with published data (**Abouelfetoh et al., 2017**), which demonstrated that by increasing the concentration of the extract gradually, the intensity of SPR increased and there was a shift towards a lower wavelength. This shift was due to a decrease in the mean size of AgNPs. On further increasing the concentration, there was a reduction in SPR intensity due to the aggregation of nanoparticles. The study depicts that even though increasing the concentration can increase the production of AgNPs, agglomeration happens beyond a threshold concentration. Agglomeration of nanoparticles can cause a reduction in their functional properties and economic importance.

Precursor Concentrations.

The size, shape, and extent of silver nanoparticle synthesis depend highly on the concentration of silver ions. Upon evaluating the effects of various concentrations of Ag⁺ ions in the reaction mixture, the absorption peak increased when the concentration of AgNO₃ risen from 0.5 to 6Mm. However, further increases in AgNO₃ concentrations up to 8mM resulted in peaks with lower Absorbance (**Fig. 6 and 7**). The maximum peak found at 4mM, 5mM, and 6Mm (OD_{450nm}~3) could be attributed to the enhancement in the oxidation of hydroxyl groups by the metal ions (**Shankar et al., 2004; Kora et al., 2010**).

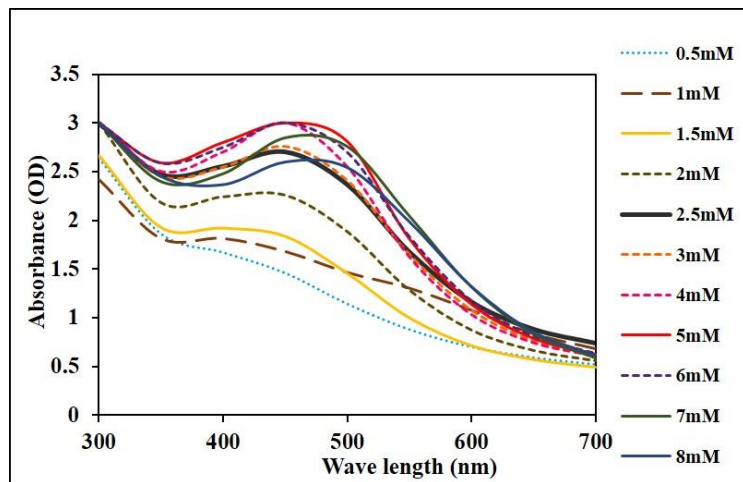


Fig. 6. UV-visible spectra of ULAgNPs at different concentrations of AgNO₃ solution.



Fig. 7. Effect of different concentrations of AgNO₃ (in mM) on ULAgNPs biosynthesis containing 5:5, v/v ratio at static conditions and 30 °C for 48 hr.

Effect of Temperature

Temperature is another significant factor that influences the biosynthesis of AgNPs. Generally, the rate of reaction and production of NPs increases with an increase in temperature (Hasan *et al.*, 2018). Moreover, temperature can also help in the higher output of NPs and regulate the size of the particles (Chugh *et al.*, 2021). The present results showed that the highest absorption peak occurred at 60 °C. Intriguingly, increasing the temperature to 70 and 80 °C resulted in peaks with lower Absorbance (Fig. 8 and 9). A probable explanation is that an increase in temperature to a certain degree activates the reductants (biomolecules) during the synthesis of NPs, while raising the temperature beyond the optimum degree could result in biomolecule degradation and the formation of agglomerated NPs or stopping the reduction reaction (Hamida *et al.*, 2023). Liu *et al.* (2020), reported that the formation of NPs at higher temperatures might be due to an increase in the nucleation kinetics constant instead of a decreased growth kinetics constant, considering the concentrations of the precursors. Also, Dong *et al.* (2014), stated that an increase in the reaction temperature caused the rapid formation of Ag clusters and reduced the concentration of the Ag precursor, and uniform AgNPs were formed with an immediate reduction rate. Rehman *et al.* (2023) observed that 70°C is the optimum temperature for AgNP formation using an extract of *Teucrium stocksianum*.

Effect of light (illumination)

Illumination is a critical physical factor affecting the synthesis of AgNPs as it can act as a catalyst for many reactions. UV-visible spectra of ULAgNPs synthesized by incubating algal extract with silver nitrate in the presence and absence of light are shown in (Fig. 10 and 11).

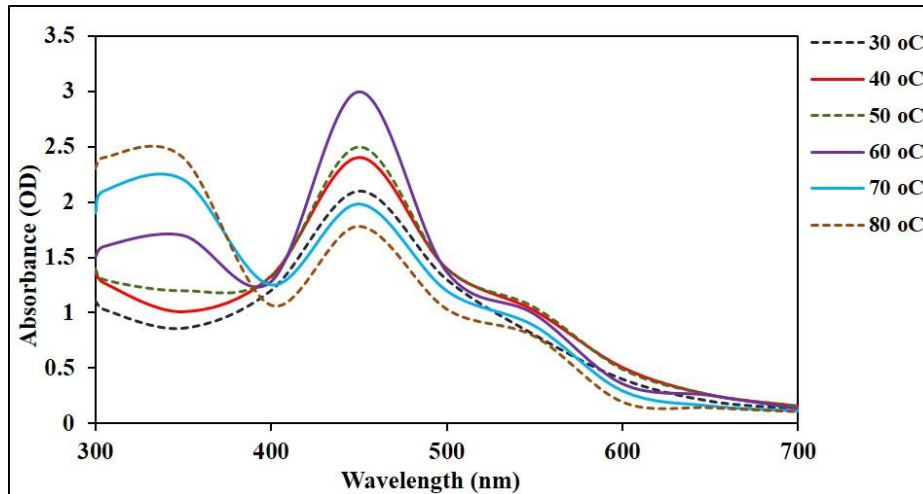


Fig.8. UV –Vis spectra of ULAgNPs at different temperatures (30-80 °C).

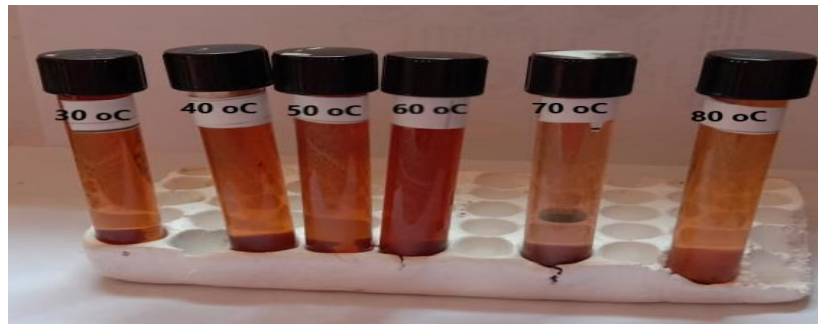


Fig.9. Effect of different temperatures (30 °C- 80 °C) on ULAgNPs synthesis in a reaction solution containing 5:5, v/v ratio of 4mM AgNO₃ and algal extract.

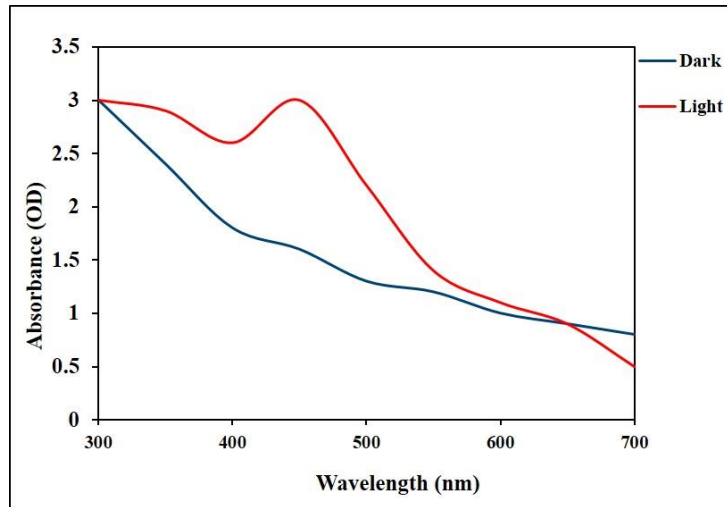


Fig.10. UV-visible spectra of ULAGNPs at dark and light conditions.



Fig. 11. Biosynthesis of ULAGNPs in reaction solution containing (5:5, v/v) ratio of 4mM AgNO₃ kept at static condition for 84h in dark and light conditions.

Higher absorbance intensity (OD 450nm~3) was recorded when the reaction mixture was incubated in light. Multiple experimental pieces of evidence establish the effect of illumination during nanoparticle synthesis. **Patel *et al.* (2015)**, in an experiment, showed that extracellular polysaccharides isolated from the *Scenedesmus sp.* were able to synthesize AgNPs in the presence of light but failed to do so in the dark, and this indicates how important light is for the synthesis of silver nanoparticles in this condition. Another group of researchers led by **Bao *et al.* (2015)**, reported the same observation by using an aqueous cell extract of *Neochloris oleoabundans*. They found that the biosynthesis of AgNPs needs white, blue, or purple light illumination. The same extract failed to show NPs synthesis when the reaction was carried out in dark conditions or in the presence of orange or red light (**Bao and Lan, 2018**). Moreover, that it is not only illumination; there are particular wavelengths that assist in the AgNPs synthesis by different methods. Even UV light can affect the size of AgNPs (**Patel *et al.*, 2015**).

Effect of pH

The pH of the reaction mixture has a significant effect on the biosynthesis of AgNPs as it alters the electrical charges of biomolecules, probably affecting their reducing and capping properties (**Azarbani and shiravand, 2020; Seifipour *et al.*, 2020**). The formation of nucleation centers, the activity of phytochemicals present in algal extract, and the rate of reduction of a metal salt are highly influenced by the pH of the solution, resulting in a change in shape and size of the nanoparticles (**Hamouda *et al.*, 2019 and Rajkumar *et al.*, 2021**). It is because the electrical charge of biomass and capping agents are altered strongly at different pH conditions, which causes alteration in their ability to bind and reduce metal ions (**Chugh *et al.*, 2021**). Varying the pH of the reaction medium leads to the synthesis of nanoparticles with various shapes and sizes.

The data of this work (**Fig. 12 and 13**) indicate that at acidic pH (4-6), no absorption peak was observed in the spectrum region, while the maximum absorption peak was at pH 8 ($OD_{450nm} \sim 3$), by increasing the pH to higher values, decrease in the absorption peak is arisen. This result agrees with data published by **Moldovan *et al.* (2018)**, who revealed that at low pH, aggregation takes place over nucleation, forming large-sized nanoparticles whereas high pH results in highly stable small-sized nanoparticles. Several reports also confirmed this result and exhibit that an acidic medium promotes the production of large-size AgNPs whereas small-size AgNPs were formed in the alkaline medium (**Siddiqui *et al.*, 2018**). In general, NPs produced in an alkaline reaction mixture are smaller and more stable in time. The reason might be the earlier capping process and is more efficient at alkaline pH values due to a large quantity of activated phytochemicals (**Miu and Dinischiotu, 2022**). Generally, NPs produced in an alkaline reaction mixture have a smaller size. They are more stable in time and this might be the capping process that occurs earlier and is more efficient at alkaline pH values due to a large quantity of activated phytochemicals.

Transmission electron microscopy (TEM)

TEM was used to ascertain the stability of the biosynthesized AgNPs, the shape, size dispersion, crystalline structure, and surface condition of the particles (**Younis *et al.*, 2021**). The findings shown in **Fig. (14)** illustrated that the ULAgNPs were distinct, regular, mostly spherical, size ranging from 4.08 - 27.57nm, and the average particle size was 10.29 nm. Our findings concurred with those reported by **El-Rafie *et al.* (2013)** who revealed that the biosynthesized AgNPs formed from polysaccharides extracted from *Ulva fasciata*, *Jania rubins*, *Pterocladia capillaceae*, and *Colpomenia sinusa* were predominantly spherical and polydispersed with maximum particle size of 7, 12, 7, and 20 nm respectively.

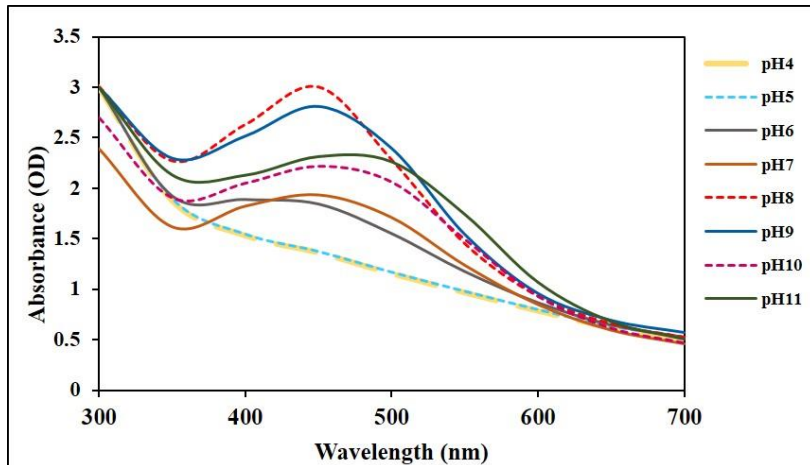


Fig. 12. UV- visible spectra of ULAgNPs synthesized at different pH values (4-11).

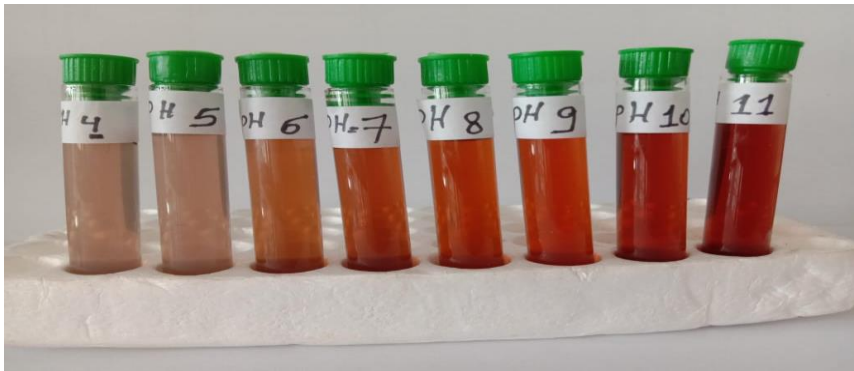


Fig. 13. Effect of different pH values (4-11) on ULAgNPs in reaction solution containing (5:5, v/v) ratio of 4mM AgNO₃ and algal extract kept at static condition in light

Our findings were also in agreement with those of **El-Sheekh *et al.* (2022)**, who discovered that the AgNPs produced using sodium alginate derived from *Sargassum latifolium* were spherical, polydispersed, and their size ranged from 4.34 - 13.77 nm with the average size 9.005nm.

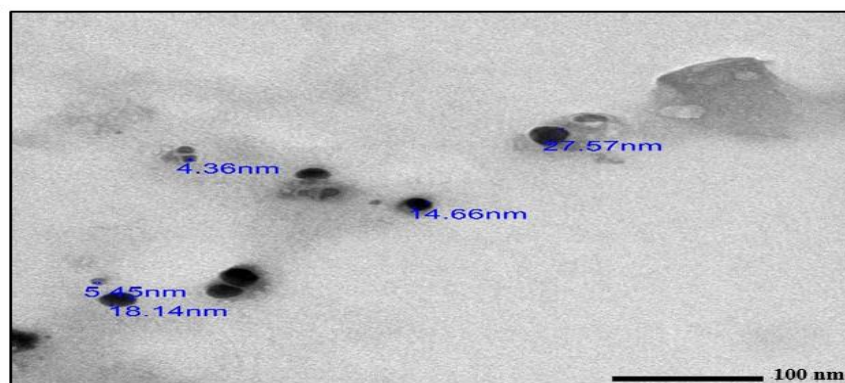


Fig. 14. Transmission electron microscopy (TEM) image of the *Ulva lactuca* mediated silver nanoparticles (ULAgNPs) (100nm), showing different particle sizes.

Biological activities

Antiviral activity of ULAGNPs

The VERO cell line (Table 1) and MTT test (Table 2) were used to assess AgNPs antiviral activity against Adenovirus. Table (1) shows the cytotoxic activity of AgNPs with Mammalian cells from African Green Monkey Kidney (Vero) cells under these experimental conditions, with a cell cytotoxic concentration (CC₅₀) of

20.34 ±0.78µg/ml. Table (2) shows that AgNPs has a weak antiviral activity (+) against Adenovirus (9.83±0.65 % inhibition). The results didn't exceed the reference drug (Amantadine).

Indeed, it was reported that AgNPs reduced the infectivity of 31 viruses belonging to 17 different virus families. The complexity of the virus structure may contribute to the limited knowledge of the mechanism of interference of nanoparticles with viruses. There are two possible methods by which AgNPs exert their antiviral activities. The first possible mechanism is that AgNPs can bind to the outer coating of proteins, suppressing the virus's attachment to cell receptors. The second possible mechanism is that AgNPs bind to nucleic acid (DNA/RNA) and inhibit the replication or proliferation of the virus inside the host cells (**Salleh *et al.*, 2020; Bamal *et al.*, 2021**). It is also evident that AgNPs can alter the structure of surface proteins, thus reducing their detection and adhesion to the host receptor (**Bamal *et al.*, 2021**).

AgNPs biosynthesized from the brown seaweed *Sargassum within* was found to AgNPs possess size-dependent interaction and the ability to block HSV-1 virus attachment and entry (**Dhanasezhian *et al.*, 2019**).

AgNPs by chemical redox method using tannic acid were reported to have antiviral activity against Adenovirus by their ability to damage the viral structure (**Chen *et al.*, 2013; Luceri *et al.*, 2023**).

Table 1. Cytotoxic activity of AgNPs against VERO cell line.

ULAgNPs conc. ($\mu\text{g/ml}$)	Viability %	Inhibitory %
0	100	0
0.25	100	0
0.5	100	0
1	99.71	0.29 ± 0.33
2	94.03	5.97 ± 0.21
3.9	86.59	13.41 ± 0.17
7.8	72.18	27.82 ± 0.65
15.6	54.93	45.07 ± 1.41
31.25	38.42	61.58 ± 1.68
62.5	27.69	72.31 ± 1.39
125	18.74	81.26 ± 1.28
250	9.63	90.37 ± 0.95
500	4.73	95.27 ± 0.41

50 % cell cytotoxic concentration (CC_{50}) = $20.34 \pm 0.78 \mu\text{g/ml}$.

Table 2. Antiviral activity of ULAgNPs against Adeno virus

Virus name	MNCC ($\mu\text{g/ml}$)	Antiviral effect (%)	Antiviral effect Qualitative	Antiviral efficacy	
				EC_{50}	SI
Adenovirus	2	9.83 ± 0.65	+	Weak activity	inactive
Amantadine Reference drug	100	64.88 ± 3.24	+++	69.46	4.74

(+): Weak antiviral activity (1-<25%)

(++): Moderate antiviral activity (25-<50%)

(+++): Good antiviral activity (50-<75%)

(++++): Excellent antiviral activity (75-100%)

MNCC: Maximum noncytotoxic concentration

EC_{50} : The dose that inhibited viral infection by 50%

SI: The selectivity index

Antioxidant activity of ULAGNPs

Determination of DPPH (2, 2-Diphenyl-1-picryl hydrazyl) radical scavenging activity

The Data recorded in **Fig.15** concerning the DPPH scavenging activity of ULAGNPs and the standard ascorbic acid revealed that ULAGNPs exhibited significant DPPH free radical scavenging activity of 79.43 ± 0.75 and 86.31 ± 0.93 at concentrations of 640 and 1280 $\mu\text{g/ml}$ respectively, with IC_{50} of 263.73 ± 9.41 ($\mu\text{g/ml}$). The antioxidant activity was less than that of conventional ascorbic acid.

The DPPH activity of the AgNPs was found to increase dose-dependently. DPPH assay is the most significant and easy method for determining antioxidant activity (**Rout *et al.*, 2012; Zain *et al.*, 2014**). The model of scavenging the stable DPPH radical is widely used to evaluate the free radical-scavenging ability of AgNPs.

DPPH• (2, 2-diphenyl-1-picrylhydrazyl) is a stable nitrogen-centered free radical whose color changes from violet to yellow up on reduction by either the process of hydrogen or electron donation scheme 1).

Antioxidant activity of AgNPs may be attributed to the functional groups adhering to AgNPs from algal extract which lead to the formation of nonreactive stable radicals by inhibiting the oxidation of molecules by preventing the initiation of chain reaction (**Arif and Uddin, 2020**). In these methods, the mechanism of antioxidant action of silver nanoparticles can be ascribed to the fact that silver can exist in two oxidation states (Ag^+ and Ag^{2+}) depending on the reaction conditions and the produced AgNPs may be able to quench free radicals by donating or accepting electrons (**Shanmugasundaram *et al.*, 2013; Bedlovicová *et al.*, 2020**). The resulting antioxidant activity of AgNPs significantly depends mainly on the reducing substances in the extract bounded/capped to the surface of the nanoparticles. Antioxidant characteristics of AgNPs were reported to rely on

chemical composition, nature, stability, surface-to-volume ratio, size, surface coating, and surface charge (Khalil *et al.*, 2020). Our results are in good agreement of that of Mohanta *et al.* (2022), who claimed that the green synthesized AgNPs from the aqueous extract of marine seaweed, *Gracilaria edulis* exhibited higher DPPH radical scavenging activity of 86.83% at a concentration of 50 $\mu\text{g/ml}$ and IC_{50} value of $30.71 \pm 0.22 \mu\text{g/ml}$. Also, AgNPs synthesized by using green algae *Spirogyra hyalina* showed potent antioxidant activity and successfully scavenged the DPPH free radicals up to $53.43 \pm 0.1731.39 \pm 0.33$, at a concentration of 400 mg/ml of nanoparticles (Abdullah *et al.*, 2021).

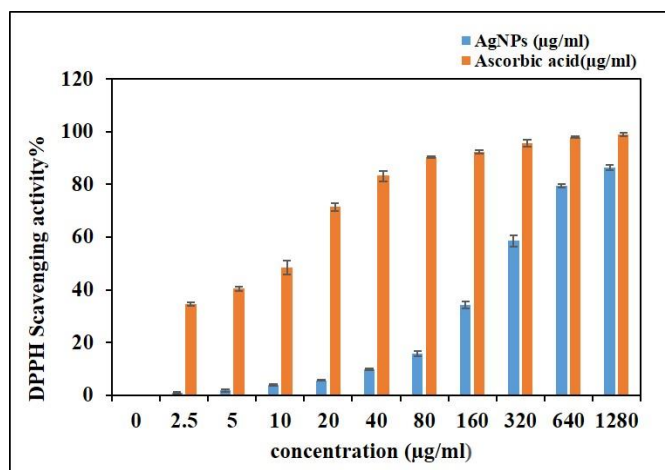
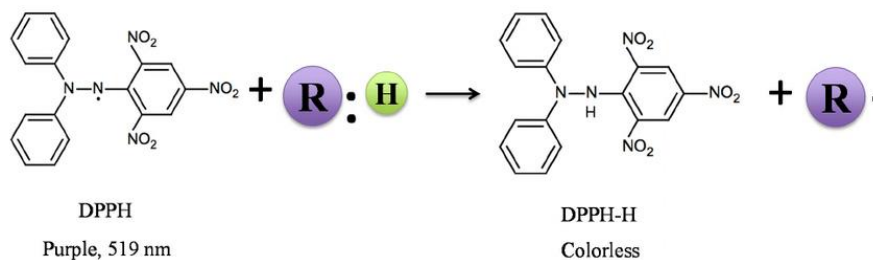



Fig.15.The effect of different concentrations of ULAGNPs on DPPH radical Scavenging activity with (IC_{50}) 263.73 ± 9.41 and 10.64 ± 0.82 for ULAGNPs and Ascorbic acid (reference drug), respectively. Each value represents the mean of the sample \pm standard deviation (SD).



 represents antioxidant

Scheme.1. Mechanism of DPPH scavenging activity

References

- Abdullah, N. S., Al-Radadi, T., Faisal, H. and Shaha, S. A. R. (2022). Novel biosynthesis, characterization and bio-catalytic potential of green algae (*Spirogyra hyalina*) mediated silver nanomaterials. *Saudi Journal of Biological Sciences*, **29**, 411–419.
- Aboelfetoh, E. F., El-Shenody, R. A. and Ghobara, M. M. (2017). Eco-friendly synthesis of silver nanoparticles using green algae (*Caulerpa serrulata*): reaction optimization, catalytic and antibacterial activities. *Environ Monit Assess*, **189**, 189(7, 7). <https://doi.org/10.1007/s10661-017-6033-0>
- Agbor, G. and Vinson, J. (2014). Folin-ciocalteau reagent for polyphenolic assay. *Int. J. Food Sci. Nutr. Diet.*, **3**, 1–19.

- Ahmad, T., Wani, I. A., Manzoor, N., Ahmed, J. and Ansari, A. M. (2013).** Biosynthesis, structural characterization and antimicrobial activity of gold and silver nanoparticles. *Colloid and Surfaces B. Biointerfaces*, **107**, 227-234.
- Aldakheel, F. M., Sayed; M. M. E., Mohsen, D., Fagir, M. H. and El Dein, D. K. (2023).** Green Synthesis of Silver Nanoparticles Loaded Hydrogel for Wound Healing; Systematic Review. *Gels*, **9**, 530. <https://doi.org/10.3390/gels9070530>.
- Aleem, A. A. (1978).** Contribution to the study of the marine algae of the red sea. I- the algae in the neighborhood of al-Ghardaqa, Egypt (Cyanophyceae, Chlorophyceae and Phaeophyceae. *Bull Fac Sci King Abdulaziz Univ Jeddah*, **2**, 73–88.
- Aleem, A. A. (1993).** Marine algae in Alexandria, Egypt. Alexandria Privately Published 1–135.
- Al-Kordy, H.M.H., Sabry, S.A. and Mabrouk, M.E.M. (2021).** Statistical optimization of experimental parameters for extracellular synthesis of zinc oxide nanoparticles by a novel haloalkaliphilic *Alkalibacillus* sp. W7. *Scientific Reports*, **11**, 10924. doi.org/10.1038/s41598-021-90408-y.
- Alzahrani, E. and Welham, K. (2014).** Optimization preparation of the biosynthesis of silver nanoparticles using watermelon and study of its antibacterial activity. *Int. J. Basic Appl. Sci.*, **3**, 392.
- Anand, G. T., Nithiyavathi, R., Ramesh, R., John Sundaram, S. and Kaviyarasu, K. (2020).** Structural and optical properties of nickel oxide nanoparticles: Investigation of antimicrobial applications. *Surf. Interfaces*, **18**, 100460.

- Arasu, M. V., Arokiyaraj, S., Viayaraghavan, P., Kumar, T. S. J., Duraipandiyar, V., Al-Dhabi, N. A. and Kaviyarasu, K. (2019).** One step green synthesis of larvicidal, and azo dye degrading antibacterial nanoparticles by response surface methodology. *J. Photochem. Photobiol. B Biol.*, **190**, 154–162. <https://doi.org/10.1016/j.jphotobiol.2018.11.020>.
- Arif, R. and Uddin, R. (2020).** A review on recent developments in the biosynthesis of silver nanoparticles and its biomedical applications. *Med Devices Sens.*, **4**: e10158. <https://doi.org/10.1002/mds3.10158>.
- Azarbani, F. and Shiravand, S. (2020).** Green synthesis of silver nanoparticles by *Ferulago macrocarpa* flowers extract and their antibacterial, antifungal and toxic effects. *GREEN CHEMISTRY LETTERS AND REVIEWS*, **13**, (1) 41–49.
- Bamal, D., Singh, A., Chaudhary, G., Kumar, M., Singh, M., Rani, N., Mundlia, P. and Sehrawat, A. R. (2021).** Silver Nanoparticles Biosynthesis, Characterization, Antimicrobial Activities, Applications, Cytotoxicity and Safety Issues: An Updated Review. *Nanomaterials*, **11**, 2086. <https://doi.org/10.3390/nano11082086>.
- Bao, Z. and Lan, C. Q. (2018).** Mechanism of light-dependent biosynthesis of silver nanoparticles mediated by cell extract of *Neochloris oleoabundans*. *Colloids Surfaces B Biointerfaces*, **170**, 251–257.
- Bedlovic'ová, Z., Strapáč, I., Baláž, M. and Salayová, A. (2010).** A Brief Overview on Antioxidant Activity Determination of Silver Nanoparticles. *Molecules*, **25**, 3191.
- Bindhu, M. R. and Umadevi, M. (2013).** Synthesis of monodispersed silver nanoparticles using Hibiscus cannabinus leaf extract and its antimicrobial activity. *Spectrochim. Acta A Mol. Biomol. Spectrosc.*, **101**, 184–190.

- Chen, N., Zheng, Y., Yin, J., Li, X., and Zheng, C. (2013).** Inhibitory effects of silver nanoparticles against adenovirus type 3 in vitro. *J. Virolo. Methods*, **193(2)**, 470–477. <https://doi.org/10.1016/j.jviromet.2013.07.020>.
- Chugh, D., Viswamalya, V. S. and Das, B. (2021).** Green synthesis of silver nanoparticles with algae and the importance of capping agents in the process. *Journal of Genetic Engineering and Biotechnology*, **19**, 126 <https://doi.org/10.1186/s43141-021-00228-w>.
- Devi, J. S., Bhimba, B. V. (2012).** Anticancer activity of silver nanoparticles synthesized by the seaweed *Ulva lactuca* in vitro. *Open Acces Sci. Re.*, **02**, 1– 5.
- Dhanasezhian, A., Srivani, S., Govindaraju, K., Parija, P., Sasikala, S. and Ramesh Kumar, M. R. (2019).** Anti-herpes simplex virus (HSV-1 and HSV-2) activity of biogenic gold and silver nanoparticles using seaweed *Sargassum wightii*. *Indian J. Geo-Mar. Sci.*, **48**, 1252–1257. [doi:10.1088/1755-1315/1110/1/012021](https://doi.org/10.1088/1755-1315/1110/1/012021).
- Dhavale, R., Jadhav, S. and Sibi, G. (2020).** Microalgae mediated silver nanoparticles (Ag-NPs) synthesis and their biological activities. *J Crit Rev*, **7(2)**, 15–20.
- Dhoble, S. M., and Kulkarni, N. S. (2016).** Biosynthesis and characterization of different metal nanoparticles by using fungi. *Scholar Academic Journal of Biosciences*, **4 (11)**, 1022-1031.
- Dipankar, C. and Murugan, S. (2012).** The green synthesis, characterization and evaluation of the biological activities of silver nanoparticles synthesized from *Iresine herbstii* leaf aqueous extracts. *Colloids Surf. B Biointerfaces*, **98**, 112–119.

- Dong, C., Zhang, X., Cai, H. and Cao, C. (2014).** Facile and one-step synthesis of monodisperse silver nanoparticles using gum acacia in aqueous solution. *J. Mol. Liq.*, **196**, 135–141.
- El-Rafie, H., El-Rafie, M., and Zahran, M. (2013).** Green synthesis of silver nanoparticles using polysaccharides extracted from marine macro algae. *Carbohydr. Polym.*, **96** (2), 403–410.
- El- Sheekh, M., Alwaleed, E. A., Kassem, W. M. A., Saber, H. (2020).** Antialgal and anticancer activities of the algal silver nanoparticles against the toxic cyanobacterium *Microcystis aeruginosa* and human tumor colon cell line. *Environ. Nanotechnol. Monit. Manag.*, **14**, 100352.
- El- Sheekh, M., Hassan, L. H., Morsi, H. H. (2021).** Assessment of the in vitro anticancer activities of cyanobacteria mediated silver oxide and gold nanoparticles in human colon CaCo- 2 and cervical HeLa cells. *Environ. Nanotechnol. Monit. Manag.*, **16**, 100556.
- El- Sheekh, M. M., Deyab, M. A., Hassan, N. I., and Abu Ahmed, S. E. (2022).** Green biosynthesis of silver nanoparticles using sodium alginate extracted from *Sargassum latifolium* and their antibacterial activity. *Rendiconti Lincei. Scienze Fisiche e Naturali*, **33**, 867–878.
- González-Ballesterosa, N., Rodríguez-Argüellesa, M. C., Prado-Lópezb, S., Lastrac, M., Grimaldid, M., Cavazzad, M. A., Nasie, L., Salviatie, G., Bigid, F. (2018).** Macroalgae to nanoparticles: Study of *Ulva lactuca* L. role in biosynthesis of gold and silver nanoparticles and of their cytotoxicity on colon cancer cell lines. *Materials Science & Engineering C*, **97**, 498–509.
- Guiry, G. M. (2020).** In: Guiry MD, Guiry GM (eds) AlgaeBase. Worldwide electronic publication. National University of Ireland, Galway. <https://www.algaebase.org>.

- Gupta, M., Tomar, R. S., Kaushik, S., Sharma, D. and Mishra, R. K. (2018).** Effective antimicrobial activity of green ZnO nanoparticles of *Catharanthus roseus*. *Frontiers in Microbiology*, **9**, 2030. DOI: 10.3389/fmicb.2018.02030.
- Hamida, R. S., Ali, M. A., Mugren, N., Al-Zaban, M. I., Bin-Meferij, M. M. and Redhwan, A. (2023).** *Planophila laetevirens*-Mediated Synthesis of Silver Nanoparticles: Optimization, Characterization, and Anticancer and Antibacterial Potentials. *ACS Omega* **8**, 29169–29188. <http://pubs.acs.org/journal/acsodf>.
- Hamouda, R. A., Hussein, M. H., Abo-elmagd, R. A., Bawazir, S. S. (2019).** Synthesis and biological characterization of silver nanoparticles derived from the cyanobacterium *Oscillatoria limnetica*. *Sci Rep.*, **9**(1), 1–17. <https://doi.org/10.1038/s41598-019-49444-y>
- Hasan, M., Ullah, I., Zulfiqar, H., Naeem, K., Iqbal, A., Gul, H., Ashfaq, M. and Mahmood. N. (2018).** Biological entities as chemical reactors for synthesis of nanomaterials: Progress, challenges and future perspective. *Mater Today Chem.*, **8**, 13–28. <https://doi.org/10.1016/j.mtchem.2018.02.003>.
- Hu, J. M. and Hsiung, G. D. (1989).** Evaluation of new antiviral agents I: in vitro prospective. *Antivir. Res.*, **11**, 217–232.
- Jakinala, P., Lingampally, N., Id, B. H., Sayyed, R. Z. (2021).** Silver nanoparticles from insect wing extract: biosynthesis and evaluation for antioxidant and antimicrobial potential. *PLoSOne*, **16** (3), 1–15.
- Kannan, R. R. R., Stirk, W. A. and Van Staden, J. (2013).** Synthesis of silver nanoparticles using the seaweed *Codium capitatum* P.C. Silva (Chlorophyceae). *South Afr J Botany*. South African Association of Botanists **86**, 1–4. <https://doi.org/10.1016/j.sajb.01.003>.

- Karmous, I., Pandey, A., Ben, K., Haj K, B., Chaoui, A. (2020).** Efficiency of the green synthesized nanoparticles as new tools in cancer therapy: insights on plant-based bioengineered nanoparticles, biophysical properties, and anticancer roles. *Bio. Tra. Ele. Res.*, **196**, 330–342.
- Khalil, I., Yehye, W. A., Etxeberria, A. E., Alhadi, A. A., Dezfooli, S. M., Julkapli, N. B. M., Basirun, W. J. and Seyfoddin, A. (2020).** Nanoantioxidants: Recent Trends in Antioxidant Delivery Applications. *Antioxidants*, **9**, 24.
- Khalil, M. M. H., Ismail, E. H., El-Baghdady, K. Z. and Mohamed, D. (2014).** Green synthesis of silver nanoparticles using olive leaf extract and its antibacterial activity. *Arab. J. Chem.*, **7**, 1131–1139.
- Khan, N. and Jameel, J. (2016).** Optimization of reaction parameters for silver from *Fusarium oxysporum* and determination of silver nanoparticles concentration. *Journal of Material Science and Engineering*, **5(283)**, 2169-0022.
- Kora, A. J., Sashidhar, R. B. and Arunachalam, J. (2010).** Gum kondagogu (*Cochlospermum gossypium*): a template for the green synthesis and stabilization of silver nanoparticles with antibacterial application. *Carbohydrate Polymers*, **82(3)**, 670-679.
- Kumar, P., Govindaraju, M., Senthamilselvi, S., Premkumar, K. (2013).** Photocatalytic degradation of methyl orange dye using silver (Ag) nanoparticles synthesized from *Ulva lactuca*. *Colloids Surf. B: Biointerfaces*, **103**, 658–661.
- Kumar, V., Singh, D. K., Mohan, S. and Hasan, S. H. (2016).** Photo-induced biosynthesis of silver nanoparticles using aqueous extract of *Erigeron bonariensis* and its catalytic activity against Acridine Orange. *J. Photochem. Photobiol. B Biol.*, **155**, 39–50.

- Liang, N. and Kitts, D. D. (2014).** Antioxidant Property of Coffee Components: Assessment of Methods that Define Mechanisms of Action. *Molecules*, **19**, 19180-19208. doi: 10.3390/molecules 191119180.
- Lipkin, Y., and Silva, P. C. (2002).** Marine algae and seagrasses of the Dahlak Archipelago, southern Red Sea. *Nova Hedwigia*, **75(1/2)**, 1–90.
- Liu, H., Zhang, H., Wang, J. and Wei, J. (2020).** Effect of temperature on the size of biosynthesized silver nanoparticle: deep insight into microscopic kinetics analysis. *Arab. J. Chem.* **13**, 1011–1019.
- Luceri, A., Francese, R., Lembo, D., Ferraris, M. and Balagna, C. (2023).** Silver Nanoparticles: Review of Antiviral Properties, Mechanism of Action and Applications. *Microorganisms*, **11**, 629. <https://doi.org/10.3390/microorganisms11030629>.
- Makhlof, M. E. M., Albalwe, F. M., Al- Shaikh, T. M., and El- Sheekh, M. M. (2022).** Suppression Effect of *Ulva lactuca* Selenium Nanoparticles (USENPs) on HepG2 Carcinoma Cells Resulting from Degradation of Epidermal Growth Factor Receptor (EGFR) with an Evaluation of Its Antiviral and Antioxidant Activities. *Appl. Sci.*, **12**, 11546. doi: 10.3390/app122211546.
- Mena, B. (2011).** The importance of nanotechnology in biomedical sciences. *J. Biotechnol. Biomater.* **1**, 105.
- Mena, F. (2013).** "When pharma meets nano or the emerging era of nanopharmaceuticals. *Pharm. Anal. Acta.* **4**, 223.
- Miu, B. A. (2022).** Dinischiotu, A. New Green Approaches in Nanoparticles Synthesis: An Overview. *Molecules*, **27**, 6472.

- Mohanta, Y. K., Mishra, A. K., Nayak, D., Patra, B., Bratovic, A., Avula, S. K., Mohanta, T. K., Murugan, K., and Saravanan, M. (2022).** Exploring Dose-Dependent Cytotoxicity Profile of *Gracilaria edulis*-Mediated Green Synthesized Silver Nanoparticles against MDA-MB-231 Breast Carcinoma. *Oxidative Medicine and Cellular Longevity*. doi.org/10.1155/2022/3863138.
- Moldovan, B., Sincari, V., Perde-Schrepler, M. and David, L. (2018).** Biosynthesis of Silver Nanoparticles Using *Ligustrum Ovalifolium* Fruits and Their Cytotoxic Effects. *Nanomaterials*, **8**, 627.
- Mosmann, T. (1983).** Rapid colorimetric assay for cellular growth and survival: application to proliferation and cytotoxicity assays. *J. Immun. Meth*, **65**, 55–63.
- Murugan, K., Samidoss, C. M., Panneerselvam, C., Higuchi, A., Roni, M., Suresh, U., Chandramohan, B., Subramaniam, J., Madhiyazhagan, P., Dinesh, D., Rajaganesh, R., Alarfaj, A. A., Nicoletti, M., Kumar, S., Wei, H., Canale, A., Mehlhorn, H., Benelli, G. (2015).** Seaweed-synthesized silver nanoparticles: an eco-friendly tool in the fight against *Plasmodium falciparum* and its vector *Anopheles stephensi*? *Parasitol. Res.* **114**, 4087 – 4097.
- Nagarajan, S. and Kuppusamy, K. A., (2013).** Extracellular synthesis of ZnO nanoparticles using seaweeds of Gulf of Mannar, India. *J. Nanobiotech.*, **11- 39**.
- Nayak, D., Minz, A. P. Ashe, S., Rauta, P. R., Kumar, M., Chopra, P., Nayak, B. (2016).** Synergistic combination of antioxidants, silver nanoparticles and chitosan in a nanoparticlebased formulation: characterization and cytotoxic effect on MCF-7 breast cancer cell lines. *J. Colloid Interface Sci.*, **470**, 142–152.

- Patel, V., Berthold, D., Puranik, P. and Gantar, M. (2015).** Screening of cyanobacteria and microalgae for their ability to synthesize silver nanoparticles with antibacterial activity. *Biotechnol Rep*, **5(1)**, 112–119.
- Pinto, R. J. B., Almeida, A., Fernandes, S. C. M., Freire, C. S. R., Silvestre, A. J. D., Neto, C. P. and Trindade, T. (2013).** Antifungal activity of transparent nanocomposite thin films of pullulan and silver against *Aspergillus niger*. *Colloids Surf. B Biointerfaces*, **103**, 143–148.
- Pinto, R. M., Diez, J. M. and Bosch, A. (1994).** Use of the colonic carcinoma cell line CaCo-2 for in vivo amplification and detection of enteric viruses. *J. Med. Virol.*, **44**, 310–315.
- Postma, P. R., Cerezo-Chinarro, O., Akkerman, R. J., Olivieri, G., Wijffels, R. H., Brandenburg, W. A., Eppink, M. H. M. (2018).** Biorefinery of the macroalgae *Ulva lactuca*: Extraction of proteins and carbohydrates by mild disintegration. *J. Appl. Phycol.*, **30**, 1281–1293.
- Rahman, A., Kumar, S. and Nawaz, T. (2020).** Biosynthesis of Nanomaterials Using Algae. *Microalgae Cultivation Biofuels Prod Elsevier Inc.* <https://doi.org/10.1016/b978-0-12-817536-1.00017-5>.
- Rajesh, S., Raja, D. P., Rathi, J., Sahayaraj, K. (2012).** Biosynthesis of silver nanoparticles using *Ulva fasciata* (Delile) ethyl acetate extract and its activity against *Xanthomonas campestris* pv. *malvacearum*. *J. Biopest.*, **5**, 119.
- Rajkumar, R., Ezhumalai, G. and Gnanadesigan, M. (2021).** A green approach for the synthesis of silver nanoparticles by *Chlorella vulgaris* and its application in photocatalytic dye degradation activity. *Environ Technol Innov*, **21**, 101282.

- Randazzo, J. W., Piqueras, J., Diaz, R., Aznar, R. and Sanchez, G. (2017).** Improving efficiency of viability-q PCR for selective detection of infectious HAV in food and water samples. *J Appl Microbiol.*, **124**, 958–964.
- Rao, B. and Tang, R. C. (2017).** Green synthesis of silver nanoparticles with antibacterial activities using aqueous *Eriobotrya japonica* leaf extract. *Adv. Nat. Sci. Nanosci. Nanotechnol.*, **8**, 015014.
- Rehman, I., Gondal, H. Y., Zamir, R., Al-Hussain, S. A., Batool, F., Irfan, A., Noreen, S., Roheen, T., Nisar, M. and Zaki, M. E. A. (2023).** Green Synthesis: The Antibacterial and Photocatalytic Potential of Silver Nanoparticles Using Extract of *Teucrium stocksianum*. *Nanomaterials*, **13**, 1343. <https://doi.org/10.3390/nano13081343>.
- Rout, Y., Behera, S., Ojha, A. K., and Nayak, P. L. (2012).** Green synthesis of silver nanoparticles using *Ocimum sanctum* (Tulsi) and study of their antibacterial and antifungal activities. *J. Microbiol. Antimicrob.*, **4(6)**, 103–109.
- Rudrappa, M., Kumar, R. S., Nagaraja, S. K., Hiremath, H., Gunagambhire, P. V., Almansour, A. I., Perumal, K., Nayaka, S. (2023).** Myco-Nanofabrication of Silver Nanoparticles by *Penicillium brasilianum* NP5 and Their Antimicrobial, Photoprotective and Anticancer Effect on MDA-MB-231 Breast Cancer Cell Line. *Antibiotics*, **12**, 567. <https://doi.org/10.3390/antibiotics12030567>.
- Salem, S. S. and Fouda, A. (2020).** Green synthesis of metallic nanoparticles and their prospective biotechnological applications: an overview. *Biological Trace Element Research*. DOI: 10.1007/s11274-016-2044-1.

- Salleh, A., Naomi, R., Utami, N. D., Mohammad, A. W., Mahmoudi, E., Mustafa, N. and Fauzi, M. B. (2020).** The Potential of Silver Nanoparticles for Antiviral and Antibacterial Applications: A Mechanism of Action. *Nanomaterials*, **10**, 1566.
- Satpathy, S., Patra, A., Ahirwar, B. and Hussain, M. D. (2019).** Process optimization for green synthesis of gold nanoparticles mediated by extract of *Hygrophila spinosa* T. Anders and their biological applications. *Phys. E Low-Dimens. Syst. Nanostruct.*, **121**, 113830.
- Seifpour, R., Nozari, M. and Pishkar, L. (2020).** Green Synthesis of Silver Nanoparticles using *Tragopogon Collinus* Leaf Extract and Study of Their Antibacterial Effects. *Journal of Inorganic and Organometallic Polymers and Materials*, **30**, 2926–2936.
- Shah, M., Fawcett, D., Sharma, S., Tripathy, S. K. and Poinern, G. E. J. (2015).** Green synthesis of metallic nanoparticles via biological entities. *Materials*, **8**(11), 7278-7308.
- Shamsuzzaman, Mashari, A., Khanam, H. and Aljawfi, R. N. (2013).** Biological synthesis of ZnO nanoparticles using *C. albicans* and studying their performance in the synthesis of steroidal pyrazolines. *Arabian Journal of Chemistry*, **10** (2), 1-7. 1530-1536.
- Shankar, S. S., Rai, A., Ahmad, A. and Sastry, M. (2004).** Rapid synthesis of Au, Ag, and bimetallic Au core- Ag shell nanoparticles using Neem (*Azadirachta indica*) leaf broth. *Journal of colloid and Interface Science*, **275**(2), 496-502.
- Shankar, S., Chorachoo, J., Jaiswal, L. and Voravuthikunchai, S.P. (2014).** Effect of reducing agent concentrations and temperature on characteristics and antimicrobial activity of silver nanoparticles. *Mater. Lett.* **137**, 160–163.

- Shanmugasundaram, T., Radhakrishnan, M. and Gopikrishnan, V. (2013).** A study of the bactericidal, anti-biofouling, cytotoxic and antioxidant properties of actinobacterially synthesized silver nanoparticles. *Colloids Surf. B Biointerfaces*, **111**, 680–687.
- Sharma, A., Sharma, S., Sharma, K. (2016).** "Algae as crucial organisms in advancing nanotechnology: a systematic review. *J. Appli. Phycol.*, **28 (3)**, 1759 – 1774.
- Siddiqui, M. N., Redhwi, H. H., Achilias, D. S., Kosmidou, E., Vakalopoulou, E. and Ioannidou, M. D. (2018).** Green Synthesis of Silver Nanoparticles and Study of Their Antimicrobial Properties. *J Polym Environ.*, **26(2)**, 423–433. <https://doi.org/10.1007/s10924-017-0962-0>.
- Singh, A. K. and Srivastava, O. N. (2015).** One-step green synthesis of gold nanoparticles using black cardamom and effect of pH on its synthesis. *Nanoscale Res. Lett.*, **10**, 1055.
- Solanki, A. D., and Patel, I. C. (2022).** *Sargassum swartzii*: A source of silver nanoparticles, synthesis and its antibacterial activity. *Egypt. J. Agric. Res.*, **100 (3)**, 394-401.
- Tahmasebi, P., Javadpour, F., and Sahimi, M. (2015).** Three- Dimensional Stochastic Characterization of Shale SEM Images. *Transp. Porous Media.*, **110**, 521–531.
- Tripathi, D. K., Ahmad, P., Sharma, S., Chauhan, D. K., Dubey, N. K. (2017).** *Nanomaterials in Plants, Algae, and Microorganisms: Concepts and Controversies*, Academic Press, Cambridge, MA, USA.

- Uzair, B., Liaqat, A., Iqbal, H., Mena, B., Razzaq, A., Thiripuranathar, G., Rana, N. F., Mena, F. (2020).** Green and Cost - Effective Synthesis of Metallic Nanoparticles by Algae: Safe Methods for Translational Medicine. *Bioengineering*, **7**, 129.
- Valsalam, S., Agastian, P., Esmail, G. A., Ghilan, A. K. M., Al- Dhab, N. A., Arasu, M. V. (2019).** Biosynthesis of silver and gold nanoparticles using *Musa acuminata* colla flower and its pharmaceutical activity against bacteria and anticancer efficacy. *J. Photochem. Photobiol. BBiol.*, **201**, 111670.
- Verma, A. and Mehata, M. S. (2016).** Controllable synthesis of silver nanoparticles using Neem leaves and their antimicrobial activity. *J. Radiat. Res. Appl. Sci.*, **9**, 109–115.
- Vijayan, P., Raghu, C., Ashok, G., Dhanaraj, S. A. and Suresh, B. (2004).** Antiviral activity of medicinal plants of Nilgiris. *Ind. J. Med. Res.*, **120**, 24–29.
- Wei, S., Wang, Y., Tang, Z., Xu, H., Wang, Z., Yang, T. and Zou, T. (2021).** A novel green synthesis of silver nanoparticles by the residues of Chinese herbal medicine and their biological activities. *RSC Adv.*, **11**, 1411–1419.
- Yen, G. C. and Duh, P. D. (1994).** Scavenging effect of methanolic extracts of peanut hulls on free radical and active oxygen species. *J. Agricult. Food Chem.*, **42**, 629–632.
- Yesilot, S., Aydin, C. (2019).** Silver nanoparticles; a new hope in cancer therapy? *East. J. Med.*, **24** (1), 111–116.

Younis, N. S., El Semary, N. A., and Mohamed, M. E. (2021). Silver nanoparticles green synthesis via cyanobacterium *Phormidium* sp.: Characterization, wound healing, antioxidant, antibacterial, and anti-inflammatory activities. *Eur. Rev. Med. Pharmacol. Sci.*, **25**, 3083–3096.

Zain, N. M., Stapley, A. G. F., and Shama, G. (2014). Green synthesis of silver and copper nanoparticles using ascorbic acid and chitosan for antimicrobial applications. *Carbohydrate Polymers*, **112**, 195–202.

النشاط المضاد للفيروسات ومضادات الأكسدة، والتخليق الأخضر، وتحسين جزيئات

الفضة النانوية المشتقة من *Ulva lactuca*

مفيده مخلوف^١، هبة دياب^١، منى مبروك^١، محمد سعد عبد الكريم^٢

١- قسم النبات والميكروبيولوجي - كلية العلوم - جامعه دمنهور

٢- قسم النبات والميكروبيولوجي - كلية العلوم - جامعه الإسكندرية

في هذه المقالة تم دراسة تخليق جسيمات الفضة النانوية من أولفا لاكتوكا مع نشاطها المضاد للفيروسات ومضادات الأكسدة. تم أيضًا تنظيم تحسين تخليق الجسيمات النانوية. تم جمع أولفا لاكتوكا في يونيو 2020، وتم إعدادها وتحسينها لتخليق جسيمات الفضة النانوية. أظهرت الجسيمات النانوية الفضية المصنعة من أولفا لاكتوكا نشاطًا كبيرًا مضادًا للأكسدة ونشاطًا سامًا للخلايا ضد خط خلايا VERO، لكن النشاط المضاد للفيروسات ضعيف ضد الفيروس الغدي. تم تقييم تأثير زمن التفاعل ومحلول نترات الفضة و مستخلص الطحالب وتركيز المادة الأولية ودرجة الحرارة والزمن والأس الهيدروجيني على تخليق جسيمات الفضة النانوية. كما تم إجراء توصيف الجسيمات النانوية المنتجة.